JOURNAL OF THEORETICAL
AND APPLIED MECHANICS
45, 1, pp. 41-51, Warsaw 2007

CONTROL AND CORRECTION OF A GYROSCOPIC PLATFORM MOUNTED IN A FLYING OBJECT

Zbigniew Koruba

Faculty of Mechatronics and Machine Buiding, Kielce University of Technology
e-mail: ksmzko@tu.kielce.pl

The work is concerned with the optimal control and correction of a three-axis gyroscopic platform fixed on board of a flying object. The deviations from the predetermined motion are minimized by means of a method of programmed control, an algorithm of the optimal correction control, and selection of optimal parameters for the gyroscopic platform.

Key words: gyroscope, optimisation, control, navigation

Notation

$\mathbf{A}$, $\mathbf{B}$ – state and control matrices, respectively; $\boldsymbol{x}$, $\boldsymbol{u}$ – state and control vectors, respectively; $\boldsymbol{x}_p$, $\boldsymbol{u}_p$ – set (programmed) state and control vectors, respectively; $\boldsymbol{u}_k$ – correction control vector; $\mathbf{K}$ – amplification matrix; $\mathbf{Q}$, $\mathbf{R}$ – weight matrices; OGP – one-axis gyroscopic platform; TGP – two-axis gyroscopic platform; FO – flying object; TTGP – three-axis gyroscopic platform; M^p_{g1}, M^p_{g2}, M^p_{g3}, M^p_{g4} – programmed control moments applied to the inner and outer frames of the respective platform gyroscopes; M^p_{k1}, M^p_{k2}, M^p_{k3} – programmed correction moments applied to the respective stabilization axes of the platform; μ_g, μ_p – damping coefficients relative to the stabilization and precession axes of the OGP; μ_c – coefficient of dry friction in the gyroscope bearings; d_c – diameter of the gyroscope bearing journal; N_c – normal reaction in the gyroscope bearings; ϑ_{gz}, ψ_{pz} – angles determining the set position of the gyroscope and the OGP axes in space, respectively; k_k, k_g, h_g – amplification coefficients of the OGP closed-loop control; J_{go}, J_{gk} – longitudinal and lateral moments of inertia of the gyroscope rotor, respectively; n_g – gyroscope spin velocity; $\varPhi_p$, ϑ_p, ψ_p – angles determining spatial position of the platform; $\varPhi_{pz}$, ϑ_{pz}, ψ_{pz} – angles determining the set position of the platform in space; p^*, q^*, r^* – angular velocities of the FO motion (kinematic interaction with the gyroscopic platform); p^*_o, q^*_o, r^*_o – amplitudes of the angular velocities p^*, q^*, r^*, respectively; ν_z – frequency of the FO board vibrations; ν_p – set frequency of the platform vibrations.

1. Introduction

Gyroscopic platforms mounted on board of flying objects, especially homing rockets and unmanned aerial vehicles, are used as a reference for navigation instruments. They also provide the input for sighting and tracing systems, target coordinators, and television cameras (Kargu, 1988; Koruba, 1999, 2001).

Consequently, gyroscopic platforms need to be characterized by high operational reliability and high accuracy in maintaining the predetermined motion. Since the operating conditions include vibrations and external disturbances, it is essential that the platform parameters be properly selected both at the design and operation stages.

This study examines applications of the three–axis gyroscopic platform to navigation, control and guidance of weapons, such as unmanned aerial vehicles and guided bombs, when pinpoint accuracy in locating a target is required.

The presented algorithm of selection of optimal control, correction and damping moments for the three-axis gyroscopic platform ensures stable and accurate platform operation even under conditions of external disturbances and kinematic interactions with the FO board.

2. Control of the gyroscopic platform position

The equations of a controlled gyroscopic platform will be written in the vector-matrix form

$$\dot{\boldsymbol{x}} = \mathbf{A}\boldsymbol{x} + \mathbf{B}\boldsymbol{u} \tag{2.1}$$

To determine the programmed controls $\boldsymbol{u}$, use a general definition, which says that the inverse problems of dynamics (Dubiel, 1973) involve estimation of the external forces acting on a mechanical system, system parameters and its constraints at which the set motion is the only possible motion of the system. In practice, the problems are frequently associated with special cases in which it is necessary to formulate algorithms determining the control forces that assure the desired motion of the dynamic system irrespective of the initial conditions of the problem, though such a procedure is not always possible.

The next step is to formulate the desired signals (Koruba, 2001). Let $\boldsymbol{u}_p$ stand for the desired (set, programmed) control vector. The control problem involves determination of the variations of components of the vector $\boldsymbol{u}_p$ in function of time, which are actually the control moments about the gyroscope axis and the motion being determined by the desired angles (ones defining the set position in space of the platform).

Now, transform Eq. (2.1) into the form

$$\mathbf{B}\boldsymbol{u}_p = \dot{\boldsymbol{x}}_p - \mathbf{A}\boldsymbol{x}_p \tag{2.2}$$

The quantity $\boldsymbol{x}_p$ in expression (2.2) is the desired state vector of the analyzed gyroscopic platform. The estimated control moments $\boldsymbol{u}_p$, are known functions of time. Here, we are considering open-loop control of a gyroscopic platfrom, the diagram of which is shown in Fig. 1.

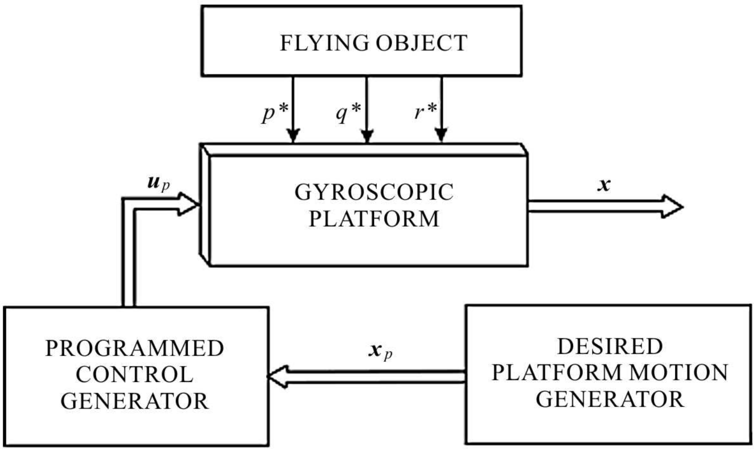

Fig. 1. Layout of the gyroscopic platform open-loop control

Now, let us check what motion of the gyroscopic platform is excited by the controls. By substituting them into the right-hand sides of Eqs. (2.2), we get

$$\dot{\boldsymbol{x}}^* = \mathbf{A}\boldsymbol{x}^* \tag{2.3}$$

where $\boldsymbol{x}^* = \boldsymbol{x} - \boldsymbol{x}_p$ is a deviation from the desired motion.

The inverse problem is explicit for the derivatives of the state variables in relation to time $\dot{\boldsymbol{x}}$, but for a fixed motion, i.e. within limits, when $t \to \infty$. The question is: will the solutions to the above equations describe also the set motion of the gyroscopic platform? If the initial axis angle is set to be the same as the required one: $x(0) = x_p(0)$, we will obtain desired angular displacements of the gyroscopic platform. However, if the initial platform position is different from the desired position, then, even though the velocities of the state variables coincide with the desired ones, the platform will not realize the desired motion in the desired location in space.

Apart from the above mentioned inconsistency of the programmed control, the platform performance is affected by external disturbances, mainly kinematic interaction with the base (flying object board), non-linear platform motion (large gyroscope axis angles), friction in the suspension bearings, manufacturing inaccuracy, errors of the measuring instruments, etc.

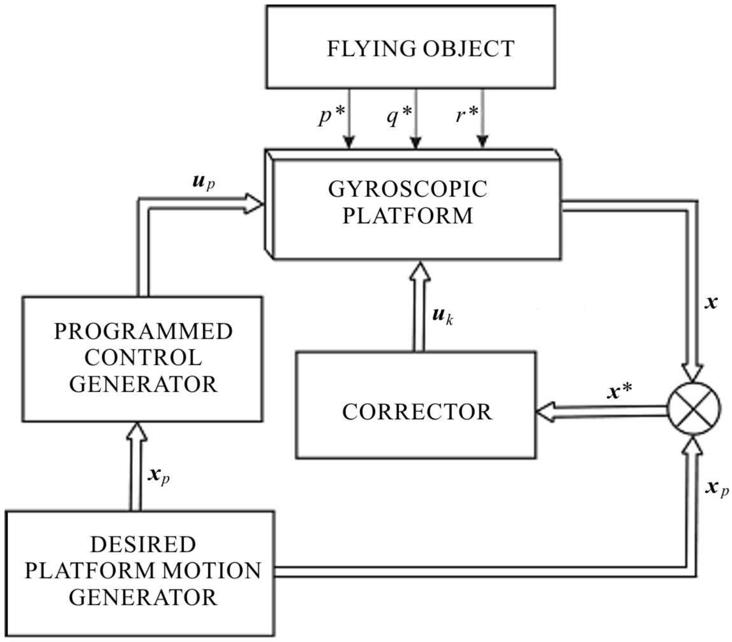

Fig. 2. Layout of the gyroscopic platform closed-loop control

Additional closed-loop correction control $\boldsymbol{u}_k$ (Fig. 2), must be applied to make the gyroscopic platform move along a set path. Then, the equations describing motion of the controlled platform will have the following form

$$\dot{\boldsymbol{x}}^* = \mathbf{A}\boldsymbol{x}^* + \mathbf{B}\boldsymbol{u}_k \tag{2.4}$$

The correction control law $\boldsymbol{u}_k$, will be determined by means of a linear-quadratic optimisation method with a functional in the form

$$J = \int\limits_0^\infty [(\boldsymbol{x}^*)^\top \mathbf{Q}\boldsymbol{x}^* + \boldsymbol{u}_k^\top \mathbf{R}\boldsymbol{u}_k]\, dt \tag{2.5}$$

The law will be presented as

$$\boldsymbol{u}_k = -\mathbf{K}\boldsymbol{x}^* \tag{2.6}$$

The coupling matrix $\mathbf{K}$ in Eq. (6) is estimated from the following relationship

$$\mathbf{A}^\top\mathbf{P} + \mathbf{PA} - 2\mathbf{PBR}^{-1}\mathbf{B}^\top\mathbf{P} + \mathbf{Q} = \mathbf{0} \tag{2.7}$$

The matrix $\mathbf{P}$ is a solution to Riccati's algebra equation

$$\mathbf{K} = \mathbf{R}^{-1}\mathbf{B}^\top\mathbf{P} \tag{2.8}$$

The weight matrices, $\mathbf{R}$ and $\mathbf{Q}$, in Eqs. (2.7) and (2.8), rearranged into the diagonal form are selected at random (Koruba, 2001), yet the search starts from the values equal to

$$q_{ii} = \frac{1}{2x_{i_{\max}}} \qquad\qquad r_{ii} = \frac{1}{2u_{i_{\max}}} \qquad\qquad i = 1,2,\dots,n \tag{2.9}$$

where: $x_{i_{\max}}$ – maximum variation range of the ith state variable value; $u_{i_{\max}}$ – maximum variation range of the ith control variable value.

By substituting (2.6) into (2.4), we obtain the equations of state in a new form again

$$\dot{\boldsymbol{x}}^* = (\mathbf{A} - \mathbf{BK})\boldsymbol{x}^* = \mathbf{A}^*\boldsymbol{x}^* \tag{2.10}$$

where

$$\mathbf{A}^* = \mathbf{A} - \mathbf{BK} \tag{2.11}$$

Recall that it is important to make the platform as stable as possible. This means the transition processes resulting from the switching on the control system or a sudden disturbance must be reduced to a minimum. Thus, selection of the optimal parameters of the system described by Eq. (2.10), and then application of the Golubiencew modified optimization method (Dubiel, 1973) are carried out.

3. Control and correction of the two- and three-axis gyroscopic platform

For a two-axis platform, the state and control vectors $\boldsymbol{x}$ and $\boldsymbol{u}$ as well as the state and control matrices $\mathbf{A}$ and $\mathbf{B}$, are as follows

$$\begin{aligned}
\boldsymbol{x} &= \Big[\vartheta_p, \frac{d\vartheta_p}{d\tau}, \psi_p, \frac{d\psi_p}{d\tau}, \vartheta_g, \frac{d\vartheta_g}{d\tau}, \psi_g, \frac{d\psi_g}{d\tau}\Big]^\top \\
\boldsymbol{u} &= [M_{k1}, M_{k2}, M_{gw}, M_{gz}]^\top \\
\mathbf{A} &= \begin{bmatrix}
0 & 1 & 0 & 0 & 0 & 0 & 0 & 0 \\
0 & -\overline{h}_{py} & 0 & 0 & 0 & \overline{\eta}_{gw} & 0 & 0 \\
0 & 0 & 0 & 1 & 0 & 0 & 0 & 0 \\
0 & 0 & 0 & -\overline{h}_{pz} & 0 & 0 & 0 & \overline{\eta}_{gz} \\
0 & 0 & 0 & 0 & 0 & 1 & 0 & 0 \\
0 & \overline{h}_{py} & 0 & -\sqrt{n} & 0 & -(\overline{\eta}_{pw} + \overline{\eta}_{gw}) & 0 & -\sqrt{n} \\
0 & 0 & 0 & 0 & 0 & 0 & 0 & 1 \\
0 & \frac{\sqrt{n}}{n} & 0 & \overline{h}_{pz} & 0 & \frac{\sqrt{n}}{n} & 0 & -(\overline{\eta}_{pz} + \overline{\eta}_{gz})
\end{bmatrix}
\end{aligned}$$

$$
\mathbf{B} = \begin{bmatrix} 0 & \overline{c}_{p1} & 0 & 0 & 0 & -\overline{c}_{p1} & 0 & 0 \\ 0 & 0 & 0 & \overline{c}_{p1} & 0 & 0 & 0 & -\overline{c}_{p2} \\ 0 & 0 & 0 & 0 & 0 & \overline{c}_{gw} & 0 & 0 \\ 0 & 0 & 0 & 0 & 0 & 0 & 0 & \overline{c}_{gz} \end{bmatrix}
$$

while

$$
\begin{array}{llll}
\tau = \Omega_g t & \Omega_g = \dfrac{J_{go} n_g}{\sqrt{J_{gw} J_{gz}}} & \overline{\eta}_{gw} = \dfrac{\eta_{gw}}{J_{gw}\Omega_g^2} & \overline{\eta}_{gz} = \frac{\eta_{gz}}{J_{gz}\Omega_g^2} \\
\overline{h}_{py} = \dfrac{h_{py}}{J_p \Omega_g} & \overline{h}_{pz} = \dfrac{h_{pz}}{J_p \Omega_g} & \overline{\eta}_{pw} = \dfrac{\eta_{pw}}{J_{pw}\Omega_g^2} & \overline{\eta}_{pz} = \dfrac{\eta_{pz}}{J_{pz}\Omega_g^2} \\
\overline{c}_{p1} = \dfrac{1}{J_{py}\Omega_g} & \overline{c}_{p2} = \dfrac{1}{J_{pz}\Omega_g} & \overline{c}_{gw} = \dfrac{1}{J_{gw}\Omega_g} & \overline{c}_{gz} = \dfrac{1}{J_{gz}\Omega_g}
\end{array}
$$

A block diagram of the control and the correction for a two-axis platform is shown in Fig. 3.

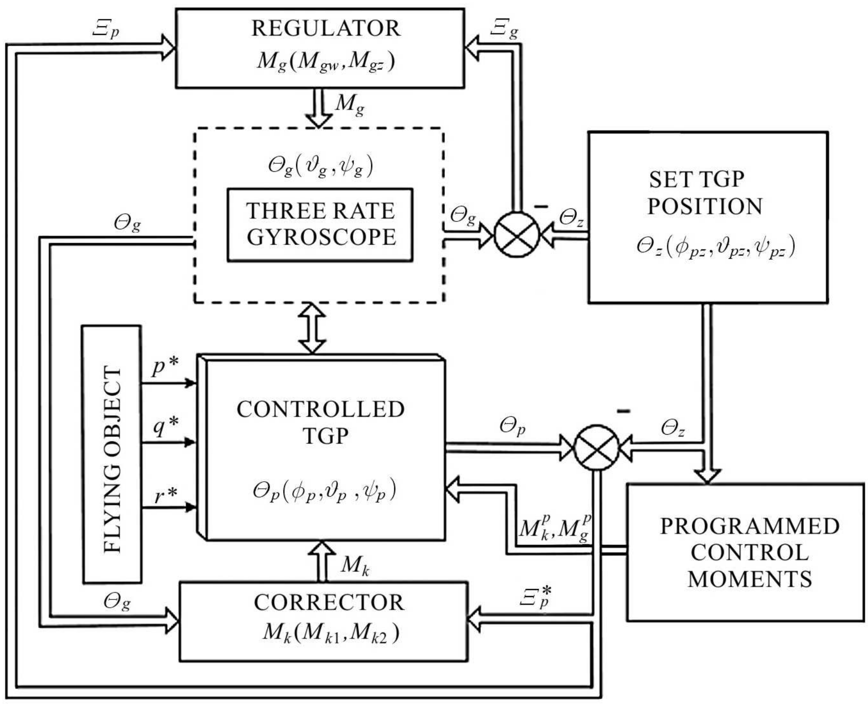

Fig. 3. Diagram of the TGP closed-loop control

However, in the case of a three-axis platform, we have

$$
\boldsymbol{x} = \Big[\psi_p, \frac{d\psi_p}{d\tau}, \vartheta_p, \frac{d\vartheta_p}{d\tau}, \Phi_p, \frac{d\Phi_p}{d\tau}, \psi_{g1}, \frac{d\psi_{g1}}{d\tau}, \vartheta_{g1}, \frac{d\vartheta_{g1}}{d\tau}, \psi_{g2}, \frac{d\psi_{g2}}{d\tau}, \vartheta_{g2}, \frac{d\vartheta_{g2}}{d\tau}\Big]^\top
$$

$$
\boldsymbol{u} = [M_{k1}, M_{k2}, M_{k3}, M_{g1}, M_{g2}, M_{g3}, M_{g3}]^\top
$$

$$
\mathbf{A} = \begin{bmatrix}
0 & 1 & 0 & 0 & 0 & 0 & 0 & 0 & 0 & 0 & 0 & 0 & 0 & 0 \\
0 & -\overline{h}_{pz} & 0 & 0 & 0 & 0 & 0 & \overline{\eta}_{p1} & 0 & 0 & 0 & 0 & 0 & \overline{\eta}_{p1} \\
0 & 0 & 0 & 1 & 0 & 0 & 0 & 0 & 0 & 0 & 0 & 0 & 0 & 0 \\
0 & 0 & 0 & -\overline{h}_{py} & 0 & 0 & 0 & 0 & 0 & \overline{\eta}_{p2} & 0 & 0 & 0 & 0 \\
0 & 0 & 0 & 0 & 1 & 0 & 0 & 0 & 0 & 0 & 0 & 0 & 0 & 0 \\
0 & 0 & 0 & 0 & 0 & -\overline{h}_{px} & 0 & 0 & 0 & 0 & 0 & \overline{\eta}_{p3} & 0 & 0 \\
0 & 0 & 0 & 0 & 0 & 0 & 0 & 1 & 0 & 0 & 0 & 0 & 0 & 0 \\
0 & \overline{h}_{pz} & 0 & A_1 & 0 & 0 & 0 & -\widehat{\eta}_{p1} & 0 & A_1 & 0 & 0 & 0 & -\overline{\eta}_{p1} \\
0 & 0 & 0 & 0 & 0 & 0 & 0 & 0 & 0 & 1 & 0 & 0 & 0 & 0 \\
0 & A_2 & 0 & 0 & 0 & A_2 & 0 & -\widehat{\eta}_{p2} & 0 & 0 & 0 & 0 & & \\
0 & 0 & 0 & 0 & 0 & 0 & 0 & 0 & 0 & 0 & 0 & 1 & 0 & 0 \\
0 & A_1 & 0 & 0 & 0 & \overline{h}_{px} & 0 & 0 & 0 & 0 & 0 & -\widehat{\eta}_{p3} & 0 & 0 \\
0 & 0 & 0 & 0 & 0 & 0 & 0 & 0 & 0 & 0 & 0 & 0 & 0 & 1 \\
0 & \overline{h}_{pz} & 0 & 0 & 0 & A_2 & 0 & -\overline{\eta}_{p1} & 0 & 0 & 0 & A_2 & 0 & -\widehat{\eta}_{p4}
\end{bmatrix}
$$

$$
A_1 = \sqrt{\frac{J_{gw}^{\Sigma}}{J_{gz}^{\Sigma}}} \qquad\qquad A_2 = -\sqrt{\frac{J_{gz}^{\Sigma}}{J_{gw}^{\Sigma}}}
$$

$$
\mathbf{B} = \begin{bmatrix}
0 & \overline{c}_1 & 0 & 0 & 0 & 0 & 0 & -\overline{c}_1 & 0 & 0 & 0 & 0 & 0 & -\overline{c}_1 \\
0 & 0 & 0 & \overline{c}_2 & 0 & 0 & 0 & 0 & 0 & -\overline{c}_2 & 0 & 0 & 0 & 0 \\
0 & 0 & 0 & 0 & 0 & \overline{c}_3 & 0 & 0 & 0 & 0 & 0 & -\overline{c}_3 & 0 & 0 \\
0 & 0 & 0 & 0 & 0 & 0 & 0 & \overline{c}_4 & 0 & 0 & 0 & 0 & 0 & 0 \\
0 & 0 & 0 & 0 & 0 & 0 & 0 & 0 & 0 & \overline{c}_5 & 0 & 0 & 0 & 0 \\
0 & 0 & 0 & 0 & 0 & 0 & 0 & 0 & 0 & 0 & 0 & \overline{c}_6 & 0 & 0 \\
0 & 0 & 0 & 0 & 0 & 0 & 0 & 0 & 0 & 0 & 0 & 0 & 0 & \overline{c}_7
\end{bmatrix}
$$

while

$$
\tau = \Omega_g t \qquad \Omega_g = \frac{J_{go} n_g}{\sqrt{J_{gw}^{\Sigma} J_{gz}^{\Sigma}}} \qquad \widehat{\eta}_{p1} = \overline{\eta}_{p1} + \overline{\eta}_{gz}
$$

$$
\widehat{\eta}_{p2} = \overline{\eta}_{p2} + \overline{\eta}_{gw} \qquad \widehat{\eta}_{p3} = \overline{\eta}_{p3} + \overline{\eta}_{gz} \qquad \widehat{\eta}_{p4} = \overline{\eta}_{p1} + \overline{\eta}_{gw}
$$

$$
\overline{\eta}_{p1} = \frac{\eta_p}{J_{pz}\Omega_g} \qquad \overline{\eta}_{p2} = \frac{\eta_p}{J_{py}\Omega_g} \qquad \overline{\eta}_{p3} = \frac{\eta_p}{J_{px}\Omega_g}
$$

$$
\overline{\eta}_{gw} = \frac{\eta_g}{J_{gw}^{\Sigma}\Omega_g} \qquad \overline{\eta}_{gz} = \frac{\eta_g}{J_{gz}^{\Sigma}\Omega_g} \qquad \overline{h}_{px} = \frac{h_{px}}{J_{px}\Omega_g}
$$

$$
\overline{h}_{py} = \frac{h_{py}}{J_{py}\Omega_g} \qquad \overline{h}_{pz} = \frac{h_{pz}}{J_{pz}\Omega_g} \qquad \overline{c}_1 = \frac{1}{J_{pz}\Omega_g^2}
$$

$$
\overline{c}_2 = \frac{1}{J_{py}\Omega_g^2} \qquad \overline{c}_3 = \frac{1}{J_{px}\Omega_g^2} \qquad \overline{c}_4 = \overline{c}_6 = \frac{1}{J_{gz}^{\Sigma}\Omega_g^2}
$$

$$
\overline{c}_5 = \overline{c}_7 = \frac{1}{J_{gw}^{\Sigma}\Omega_g^2}
$$

Figure 4 shows a layout of the control and the correction of a three-axis gyroscopic platform.

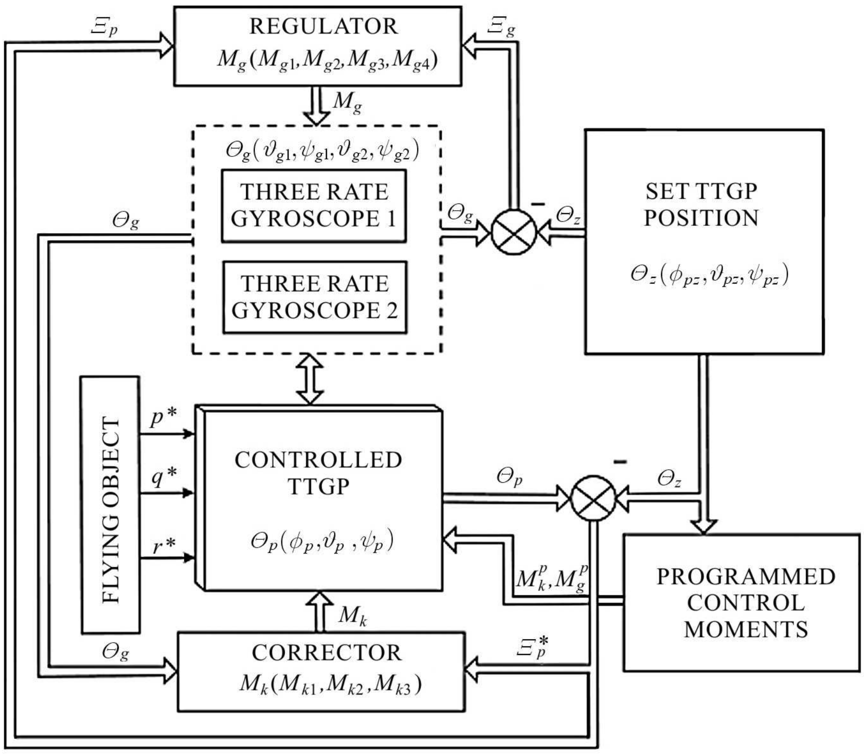

Fig. 4. Outline of the TTGP closed-loop control

4. Obtained results and conclusions

Assume that the set motion of the TGP is described by the following functions of time (the programmed motion is set around the circumference)

$$\psi_{pz} = \psi_{pz}^o \sin \nu_p t \qquad \vartheta_{pz} = \vartheta_{pz}^o \cos \nu_p t$$

and that there is an external disturbance (kinematic interaction with the base along the Ox_p, Oy_p, Oz_p axes in the form of the FO board harmonic vibrations) in the time interval $\Delta = \langle t_1, t_2 \rangle$ occurring with angular velocity equal to

$$\psi_{pz}^o = 0.25\,\text{rad} \qquad \vartheta_{pz}^o = 0.25\,\text{rad} \qquad \nu_p = 1.5\frac{\text{rad}}{\text{s}}$$
$$r_o^* = 5\frac{\text{rad}}{\text{s}} \qquad \nu_z = 50\frac{\text{rad}}{\text{s}}$$

and the disturbing moments act only in relation to the precession axis and have the form

$$M_z = M_z^v + M_z^t = \mu_g r_s + m_c^t \,\text{sgn}\,(r_s)$$

where: $m_c^t = 0.5 d_c \mu_c N_c$, with the TGP parameters equal to

$$J_{go} = 5 \cdot 10^{-3}\text{kgm}^2 \qquad J_{gk} = 2.5 \cdot 10^{-4}\text{kgm}^2 \qquad J_p = 2.5 \cdot 10^{-2}\text{kgm}^2$$

$$n_g = 600\frac{\text{rad}}{\text{s}} \qquad \mu_g = 0.01\,\text{Nms} \qquad m_c^t = 2 \cdot 10^{-4}\,\text{Nms}^2$$

Figures 5 through 8 concern the investigations of the two-axis gyroscopic platform case. We confirm the operational efficiency of the closed-loop optimal control which minimizes the deviations from the set motions to admissible values and kinematic interaction with the base (the flying object board). As there is great similarity between the TGP and TTGP cases, no data concerning the latter have been included.

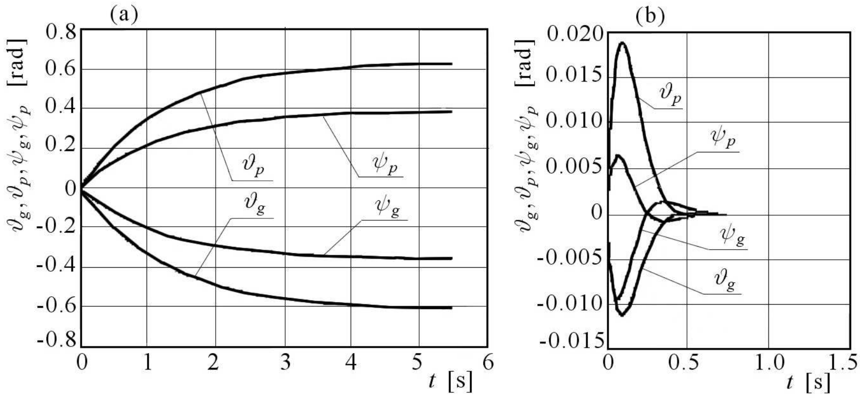

Fig. 5. Variations of the TGP angular position in function of time caused by initial conditions: (a) without correction control, (b) with correction control

The work discusses the results of some preliminary investigations of dynamics and control of a two- and three-axis gyroscopic platform fixed on board of a flying object. To realize the programmed motion of the platform, we need to apply controls determined from the inverse problem of dynamics. Then to correct and stabilize this motion, we have to introduce control with feedback. Furthermore, it is required that the Golubiencew modified method be used to determine the optimal parameters of that system.

The optimized parameters of the controlled one-, two-, and three-axis gyroscopic platform allows us:

a) to reduce the transition process to minimum;
b) to minimize the overload acting on the platform;
c) to minimize values of the gyroscope control moments, which may affect technical realizability of the control.

It should be noted that the data were obtained for two- and three-axis platforms with three-rate gyroscopes. Such gyroscopes are used as control

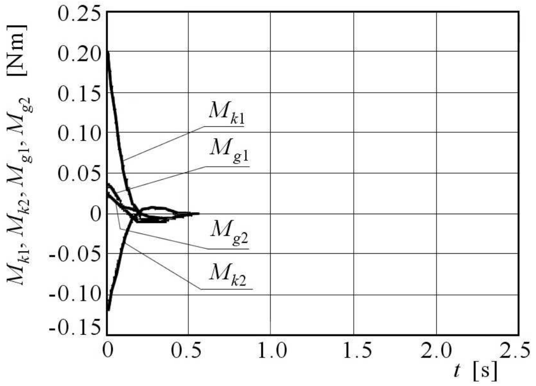

Fig. 6. Time-dependent variations of the TGP correction moments

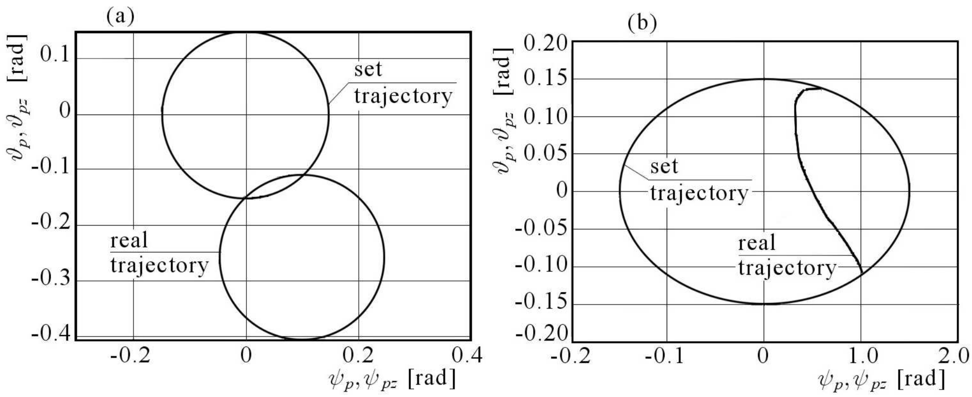

Fig. 7. The set and desired trajectories of undisturbed TGP motion: (a) in the open system, (b) with feedback

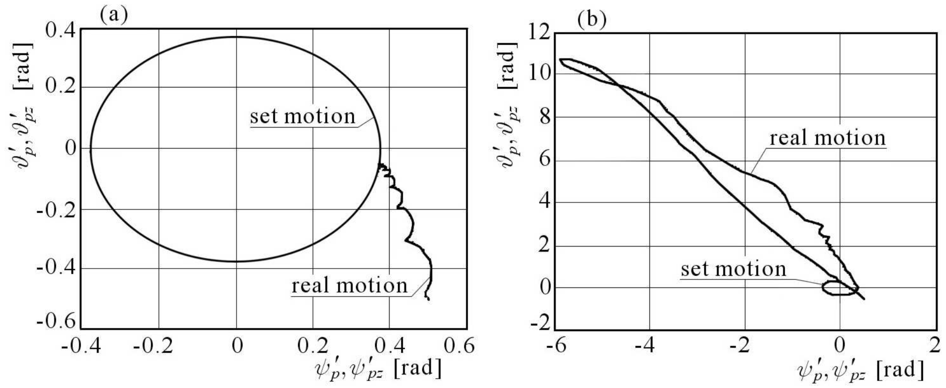

Fig. 8. The set and real undisturbed TGP motion: (a) in the open system, (b) with feedback

sensors. Thus, the operational accuracy of the platforms depends mainly on the operational accuracy of the applied gyroscopes. Since three-rate gyroscopes are easier to control, relatively little energy needs to be supplied to alter the spatial position of the platform (Koruba, 2001).

References

1. Dubiel S., 1973, Generalized constraints and their application to the study of controllability of flying objects [in Polish], *Supplement Bulletin of Military University of Technology*, Warsaw
2. Kargu L.I., 1988, *Gyroscopic Equipments and Systems*, Sudostroyenye, Leningrad
3. Koruba Z., 2001, *Dynamics and Control of Gyroscope on the Board of Aerial Vehicle* [in Polish], Monographs, Studies, Dissertations No. 25, Kielce University of Technology, p. 285, Kielce
4. Koruba Z., 1999, Selection of the optimum parameters of the gyroscope system on elastic suspension in the homing missile system, *Journal of Technical Physics*, **40**, 3, 341-354

Sterowanie i korekcja platformy giroskopowej umieszczonej na pokładzie obiektu latającego

Streszczenie

W pracy przedstawione jest sterowanie optymalne i korekcja trzyosiowej platformy giroskopowej, umieszczonej na pokładzie obiektu latającego. Odchylenia od ruchu zadanego są minimalizowane za pomocą sterowania programowego, algorytmu optymalnego sterowania korekcyjnego oraz wyboru optymalnych parametrów platformy giroskopowej.

Manuscript received August 3, 2006; accepted for print October 4, 2006